

yield a similar curve for this system.

The authors would like to thank Dr. Ron Phaneuf for several helpful discussions. Theoretical work was done under the U. S. Department of Energy Contract No. E(04-3)-115, P/A No. 111; experimental work was done under the U. S. Department of Energy Contract No. W-7405-Eng-48.

<sup>1</sup>L. P. Presnyakov and A. D. Ulantsev, *Kvant. Elektron.* **1**, 1320 (1974) [*Sov. J. Quant. Electron.* **4**, 2377 (1975)].

<sup>2</sup>R. E. Olson and A. Salop, *Phys. Rev. A* **14**, 579 (1976).

<sup>3</sup>T. P. Grozdanov and R. K. Janev, *Phys. Rev. A* **17**, 880 (1978).

<sup>4</sup>A. Müller and E. Salzborn, *Phys. Lett.* **62A**, 391 (1977).

<sup>5</sup>D. H. Madison and E. Merzbacher, in *Atomic and Inner Shell Processes*, edited by B. Crasemann (Academic, New York, 1977), pp. 1-72.

<sup>6</sup>L. D. Gardner, J. E. Bayfield, P. M. Koch, H. J. Kim, and P. H. Stelson *Phys. Rev. A* **16**, 1415 (1977).

<sup>7</sup>R. E. Olson and A. Salop, *Phys. Rev. A* **16**, 531 (1977).

<sup>8</sup>R. A. Phaneuf, F. W. Meyer, R. H. McKnight, R. E. Olson, and A. Salop, *J. Phys. B* **10**, L425 (1977).

<sup>9</sup>R. Abrines and I. C. Percival, *Proc. Phys. Soc., London* **88**, 873 (1966).

<sup>10</sup>D. R. Bates and G. Griffing, *Proc. Phys. Soc., London (Sect. A)* **66**, 961 (1953).

<sup>11</sup>K. H. Berkner, W. G. Graham, R. V. Pyle, A. S. Schlachter, J. W. Stearns, and R. E. Olson, *J. Phys. B* **11**, 875 (1978).

<sup>12</sup>K. H. Berkner, W. G. Graham, R. V. Pyle, A. S. Schlachter, and J. W. Stearns, to be published.

<sup>13</sup>H. J. Kim, F. W. Meyer, R. A. Phaneuf, P. H. Stelson, and P. Hvelplund, *Bull. Am. Phys. Soc.* **23**, 531 (1978), and private communication.

<sup>14</sup>A. B. Wittkower, G. Ryding, and H. B. Gilbody, *Proc. Phys. Soc., London* **89**, 541 (1966).

<sup>15</sup>H. B. Gilbody and A. R. Lee, *Proc. Roy. Soc. London, Ser. A* **274**, 365 (1963).

<sup>16</sup>H. B. Gilbody and J. V. Ireland, *Proc. Roy. Soc. London, Ser. A* **277**, 137 (1964).

<sup>17</sup>R. A. Phaneuf, F. W. Meyer, and R. H. McKnight, *Phys. Rev. A* **17**, 534 (1978).

<sup>18</sup>H. J. Kim, R. A. Phaneuf, F. W. Meyer, and P. H. Stelson, *Phys. Rev. A* **17**, 854 (1978). Figure 6 of this publication shows the ratio of  $\sigma_{CX}$  in H<sub>2</sub> and H for Si ions, averaged over charge states 2-9, to be  $2.0 \pm 0.3$  for relative velocities  $v \geq 4 \times 10^8$  cm/sec.

<sup>19</sup>J. W. Hooper, E. W. McDaniel, D. W. Martin, and D. S. Harmer, *Phys. Rev.* **121**, 1123 (1961).

<sup>20</sup>L. I. Pivovarov and Yu. Z. Levchenko, *Zh. Eksp. Teor. Fiz.* **52**, 42 (1967) [*Sov. Phys. JETP* **25**, 27 (1967)].

<sup>21</sup>R. A. Langley, D. W. Martin, D. S. Harmer, J. W. Hooper, and E. W. McDaniel, *Phys. Rev.* **136**, A379 (1964).

<sup>22</sup>L. I. Pivovarov, Yu. Z. Levchenko, and A. N. Grigor'ev, *Zh. Eksp. Teor. Fiz.* **54**, 1310 (1968) [*Sov. Phys. JETP* **27**, 699 (1968)].

<sup>23</sup>L. V. Puckett, G. O. Taylor, and D. W. Martin, *Phys. Rev.* **178**, 271 (1969).

<sup>24</sup>N. Bohr and J. Lindhard, *K. Dan. Vidensk. Selsk., Mat.-Fys. Medd.* **28**, 1 (1954).

<sup>25</sup>E. Merzbacher and H. W. Lewis, in *Encyclopedia of Physics*, edited by S. Flügge (Springer-Verlag, Berlin, 1958), Vol. 34, p. 166.

## High-Temperature, High-Density Plasma Production by Vortex-Ring Compression

D. R. Wells, J. Davidson, L. G. Phadke, J. G. Hirschberg, P. E. Ziajka, and J. Tunstall

*Department of Physics, University of Miami, Coral Gables, Florida 33124*

(Received 13 October 1977)

The TRISOPS III machine at the University of Miami has been modified by improving the preionization of the plasma and increasing the ring frequency of the conical  $\theta$ -pinch coils. The secondary magnetic compression field has been increased to 120 000 G at the conjugate points of the mirror. It has been possible, with this modified machine, TRISOPS IV, to obtain ion temperatures of 5 keV with corresponding electron temperature of less than 300 eV. The electron density was  $2 \times 10^{17}$  cm<sup>-3</sup>. This plasma was held in stable equilibrium for 5  $\mu$ sec.

Previous efforts to produce a high-temperature, high-density plasma by vortex-ring compression have been described elsewhere.<sup>1</sup> A schematic diagram of the machine used to produce and heat the plasma is shown in Fig. 1. Two conical  $\theta$  pinches were placed at the conjugate points of a

primary magnetic mirror guide field with a mirror ratio of 1.2. The vacuum system was constructed of ceramic in the region of the conical coils and preionization coils, and Pyrex in the region of the pumping port and optical access window at the center of the machine. Preioniza-

tion was accomplished by single-turn coils, placed close to the pinch coils, which were energized by single individual 1- $\mu$ F, 30-kV capacitors. The conical  $\theta$ -pinch coils were energized by single individual 1.5- $\mu$ F, 30-kV capacitors directly coupled to the coils. The vacuum chamber starting at a base pressure of  $2 \times 10^{-6}$  Torr was filled to a pressure of 300  $\mu$ m with deuterium.

It is now well known that each half-cycle of the current oscillation of each conical  $\theta$ -pinch coil produces a plasma vortex ring.<sup>2-5</sup> Every other ring produced by each conical pinch coil is not in equilibrium and breaks up. The remaining rings from each coil are either all corotational or contrarotational<sup>4,5</sup> (have their magnetic induction and mass velocity fields parallel or anti-parallel, respectively) and coalesce to form one strong corotational or contrarotational ring. These two

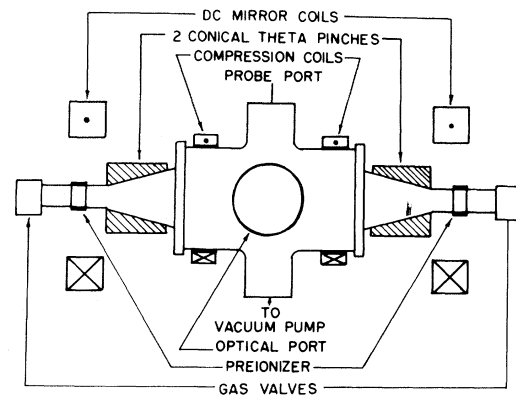


FIG. 1. Schematic diagram of machine used for secondary compression of plasma vortex structures. Primary mirror field strength was 500 G.

coalesced rings then move to the center of the primary guide field mirror and collide.

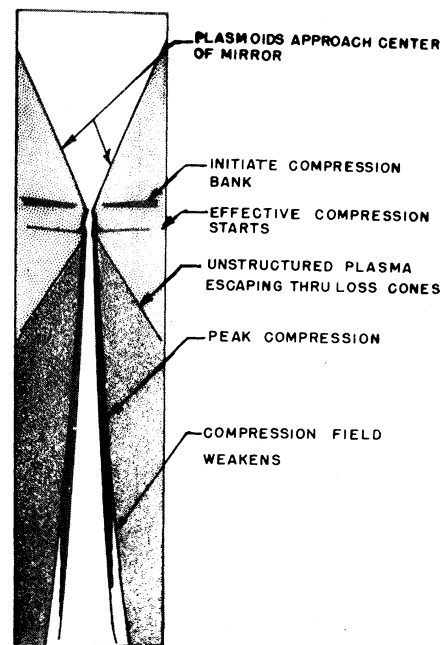
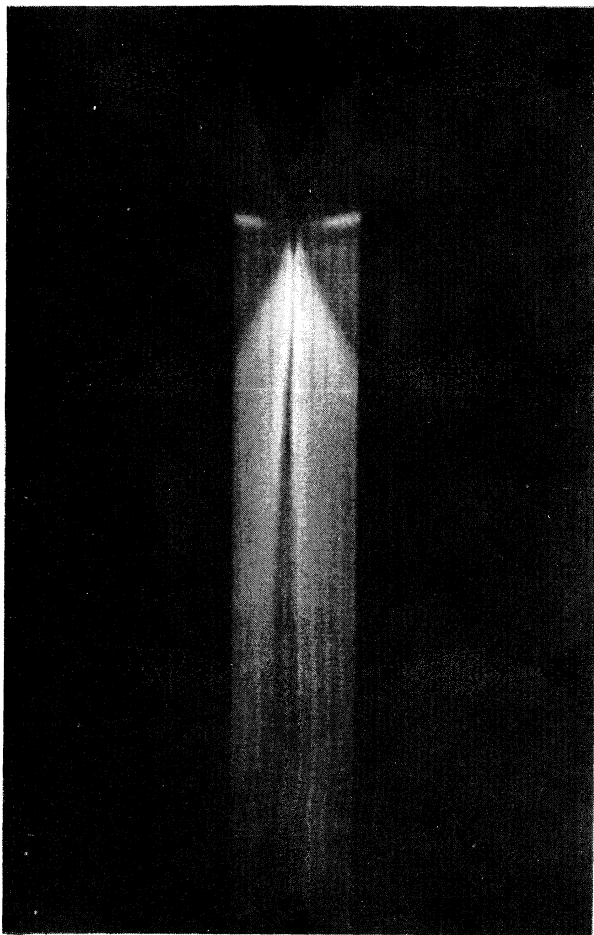


FIG. 2. Streak picture and schematic diagram illustrating collision of vortex structures at center of secondary mirror system. Time goes from top to bottom of the picture and diagram. Streak time is 50  $\mu$ sec. The horizontal slit was placed along the centerline of the machine, between the secondary compression coils.

Since they are corotational and contrarotational, they do not coalesce but interact, forming a magnetic barrier or septum which keeps each composite ring from overlapping with the other.<sup>4-7</sup> This is illustrated in Fig. 2.

After collision, the rings are stationary in the laboratory frame of reference. A secondary magnetic mirror (Fig. 1) is now used to compress and heat the vortex structures. In results previously reported, ion temperatures  $T_i = 180$  eV with corresponding electron temperatures  $T_e = 30$  eV were obtained during compression. The electron density was  $1 \times 10^{16}$  particles/cm<sup>3</sup> and the compressed rings remained in stable equilibrium for about 18  $\mu$ sec.

In the new machine, TRISOPS IV, the preionizer coils and conical  $\theta$  pinches are energized collector plates which allow higher ring frequencies. The secondary mirror coils have been decreased in diameter from 12.5 to 8.8 cm, in order to produce higher compression fields with the same capacitor bank (240 000 J at 20 kV). The machine is again run in the static mode by filling the vacuum chamber with 300  $\mu$ m of deuterium and then sealing off the system. The preionizer consists of a single-turn coil energized by a single GE clamshell capacitor. This system rings at 500 kHz. The capacitors are charged to 20 kV. The conical  $\theta$  pinches are powered by GE 1.5- $\mu$ F, 30-kV energy-storage capacitors. The current oscillates in this circuit at 450 kHz for 6  $\mu$ sec. The compression mirror coils have a quarter-cycle rise time of 10  $\mu$ sec. They are crowbarred at peak current to give an effective "field on" time of 5  $\mu$ sec. The large mirror coils, which act as a guide field for the plasma rings before compression, are powered by a rectifier and maintain a steady magnetic field of 500 G (mirror ratio is 2.8).

The preionizer coils are energized first. After 2  $\mu$ sec, the conical  $\theta$ -pinch coils are activated. 8  $\mu$ sec later, the compression field coils are energized. Exact timing of the compression coils is adjusted by observation of streak pictures of the discharge. The compression field must be activated about 1  $\mu$ sec before the rings reach the center of the mirror for best results.

Ion temperatures in the rings after they meet at the center of the primary mirror but before secondary compression are approximately 350 eV in the currently operating machine, TRISOPS IV. The electron temperature is very low ( $T_e \approx 30$  eV) and the density is typically  $10^{16}$  particles/cm<sup>3</sup>. The septum and the rings are observable for

about 30  $\mu$ sec after they meet at the center of the mirror if no secondary compression is applied. It is believed that the precompression ion temperature can easily be increased into the keV range with suitably designed conical  $\theta$  pinches energized by Marx capacitor banks. When the coalesced rings are compressed, the ion temperature rises into the keV range. Results are shown in Fig. 3. Ion temperatures as high as 5.0 keV have been measured optically with use of the 4686- $\text{\AA}$  He II line and C III and C IV lines at 3170 and 3936  $\text{\AA}$ , respectively. These ion temperatures were measured by observation of Doppler broadening of spectral lines.<sup>8</sup>

Temperature measurements have also been made by observing the neutron flux from the fireball. Neutron flux measurements were obtained by activation of metal foils fabricated from various elements with known neutron cross sections for fast and slow neutrons. Temperature obtained

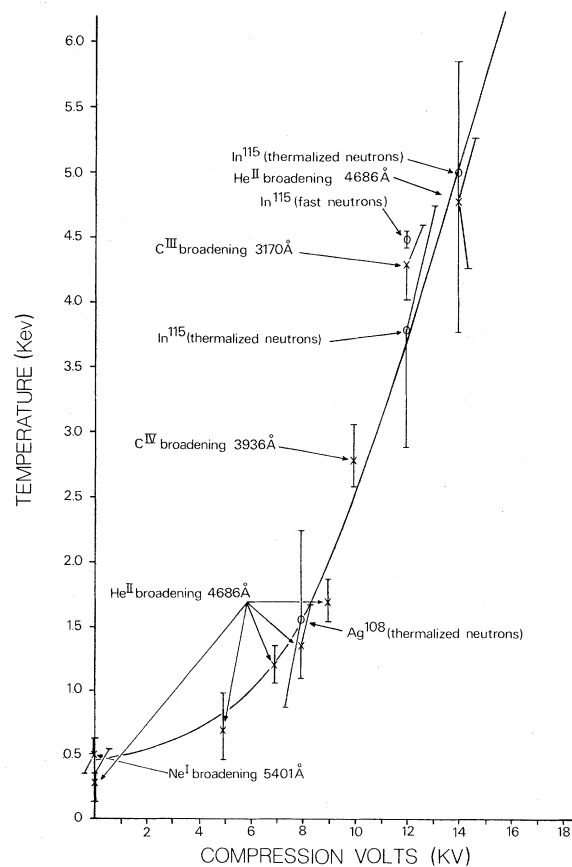


FIG. 3. Ion temperature of deuterium vs voltage applied to capacitor bank that powers the secondary mirror coils. The temperatures were measured with a multichannel monochromator.

by using neutron flux measurements fall on the temperature curve obtained by optical measurements of Doppler broadening of spectral emission lines. (See Fig. 3.) Total integrated neutron flux is  $10^8$  neutrons per shot.

Density measurements have been made utilizing the Stark broadening of spectral lines.<sup>9</sup> When ion temperatures are not precisely known, measurements are made on the line profiles of two hydrogenic spectral lines with greatly different sensitivity to Stark effect. It is then possible to solve simultaneously for the contribution because of Doppler and Stark broadening and thereby obtain both the ion temperature and electron density.<sup>9</sup> The initial data are presented in Fig. 4, which is a plot of plasma density in the fireball versus compression. When the ion temperatures determined by neutron fluxes are compared to temperatures obtained with the monochromator, a plasma density of about  $10^{17}$  at 12 kV on the bank gives an excellent fit to the "neutron" temperature data.

Plasma volume was remeasured using streak and framing camera images over several hundred shots. The results are shown in Fig. 5. An attempt to measure electron temperature with metal-foil absorbers in front of x-ray film yielded the result that  $T_e < 300$  eV. A rough check on this using line ratio techniques has been attempted. The ratio of C III to C II was used, assuming local thermodynamic equilibrium. The results indicate a  $T_e$  of less than 50 eV. High ion temperatures and electron temperatures of less than 300 eV have been attained. This is characteristic

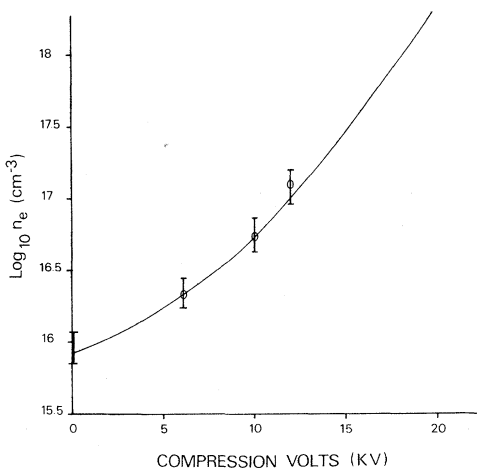


FIG. 4. Plasma density vs compression bank voltage based on Doppler- and Stark-broadening measurements.

of  $\theta$  pinches and mirror compression devices. The large difference between the magnetic pressure at the center of the mirror and the pressure in the quasi-force-free core requires explanation. For equilibrium,

$$0 = -\nabla(p + \frac{1}{2}\rho v^2) + \vec{j} \times \vec{B} - \rho(\vec{\zeta} \times \vec{v}),$$

where  $p$  = pressure,  $\rho$  = mass density,  $v$  = velocity of center of mass of a fluid element,  $\vec{j}$  = current density,  $\vec{B}$  = magnetic induction field,  $\vec{\zeta} = \nabla \times \vec{v}$ .

For force-free collinear flow with the ions carrying the conduction current, the equation takes the form

$$\nabla p + \frac{1}{2}\nabla(\rho v^2) = 0.$$

Measured velocity is close to sound speed ( $|\vec{v}| \approx 6 \times 10^5$  m/sec). A force balance is obtained in which hydrodynamic (kinetic) pressure supports the hot gas. The relatively low magnetic field merely guides the flow. The force bearing shell is the gun itself. ( $|\vec{B}|$  and  $|\vec{v}|$  are a maximum at the boundary.)

Estimates of particle confinement time at high temperatures are given by the "time one" of the ionized light used in making temperature measurements and the duration of the image on

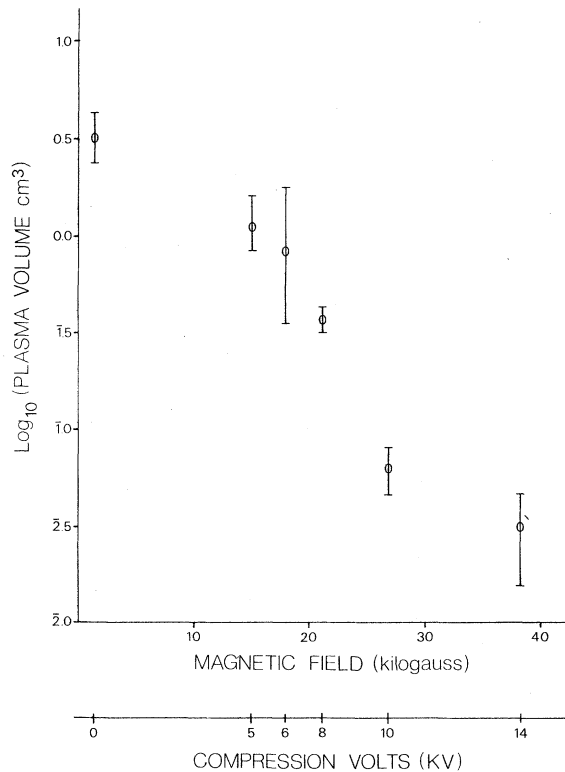


FIG. 5. Plasma volume vs compression bank voltage.

streak pictures. By both methods, the decay time of the measured  $T_i$  is 5  $\mu\text{sec}$ . The compression field is effectively at close to peak value for about 5  $\mu\text{sec}$ . The ion electron equilibration time for these structured plasmas is evidently greater than 4  $\mu\text{sec}$  at 5 keV. The fast moving ( $|\vec{v}| \approx 4 \times 10^5$  m/sec) ions are cooled by the cold electrons which act as field particles whose center of mass is stationary in the laboratory frame. The corresponding equilibration time for the compressed plasma is of the order of microseconds.<sup>10</sup>

This work was supported by the National Science Foundation, Grants No. GP-43733, No. PHY74-08237, and No. PHY77-07106, and the Florida Power and Light Company.

<sup>1</sup>D. R. Wells *et al.*, Phys. Rev. Lett. **33**, 1203 (1974).

<sup>2</sup>D. R. Wells, Phys. Fluids **5**, 1016 (1962).

<sup>3</sup>D. R. Wells, J. Plasma Phys. **4**, 645 (1970).

<sup>4</sup>D. R. Wells and J. Norwood, Jr., Phys. Fluids **3**, 21 (1969).

<sup>5</sup>D. R. Wells, in *Proceedings of Third Topical Conference on Pulsed High Beta Plasmas, UKAEA Culham Laboratory, September 1975* (Pergamon, New York, 1975).

<sup>6</sup>D. R. Wells, Phys. Fluids **7**, 826 (1964).

<sup>7</sup>J. Davidson *et al.*, "The Interaction between Two Force-Free Plasma Vortices in the TRISOPS III Machine" (to be published).

<sup>8</sup>J. Davidson *et al.*, "Simultaneous Electron Density and Ion Temperature Measurements of a Moderately Dense Plasma Using Doppler and Stark Broadened He II Lines" (to be published).

<sup>9</sup>L. G. Phadke *et al.*, "A Multi-channel Monochromator for Measurement of Electron Density and Doppler Ion Temperature on the TRISOPS Facility" (to be published).

<sup>10</sup>D. J. Rose, *Plasmas and Controlled Fusion* (M.I.T. Press, Cambridge, Mass., 1961).

## Observation of Stimulated Raman Backscatter from a Prefomed, Underdense Plasma

R. G. Watt, R. D. Brooks, and Z. A. Pietrzyk  
*University of Washington, Seattle, Washington 98195*  
 (Received 8 May 1978)

Observations of stimulated Raman backscatter in an underdense hydrogen plasma are reported. The wavelength shift associated with the backscattered Raman component is consistent with a plasma with the measured electron density. The Raman backscatter is seen to decrease below detectable levels when the incident  $\text{CO}_2$ -laser intensity is attenuated approximately 50%, consistent with theoretical intensity thresholds of the Raman process.

The problem of parametric instabilities in plasma has been examined extensively in the literature.<sup>1-7</sup> Two types of solutions emerge, characterized by an infinite, homogeneous plasma<sup>1-3</sup> or finite, inhomogeneous plasma.<sup>4-6</sup> In the infinite, homogeneous case, the three-wave interaction takes place throughout the entire plasma, and the applicable controlling equations can be solved to find threshold intensities and growth rates. The growth is primarily temporal but may have a spatial gain associated with it (absolute instability) in some circumstances. In the finite inhomogeneous case the interaction is treated as a local phenomenon which grows in space (convective instability). Here also in some instances there may be both spatial and temporal growth. Both approaches predict a number of different instabilities. The decay of an incident photon into a backscattered photon and an ion-

acoustic wave [stimulated Brillouin scattering (SBS)] has been observed in numerous experiments, primarily in Nd:glass-laser-heated solid targets<sup>8,9</sup> and in  $\text{CO}_2$ -laser-heated linear devices.<sup>10-12</sup> Decay of an incident photon into two electron plasma waves (two-plasmon decay mode)<sup>13</sup> or into one electron-plasma wave and one ion-acoustic wave (parametric decay mode)<sup>14</sup> have also been observed. The observation reported here is the decay of an incident photon into a backscattered photon and an electron plasma wave [stimulated Raman scattering (SRS)]. Stimulated Raman backscatter is characterized by an exponential backscattered-intensity dependence on the incident intensity and a backscattered frequency which is shifted to a lower frequency than the incident frequency by the electron plasma frequency  $\omega_p = (e^2 n_e / \epsilon_0 m_e)^{1/2}$ . Possible indirect evidence of the Raman process has been reported in the liter-

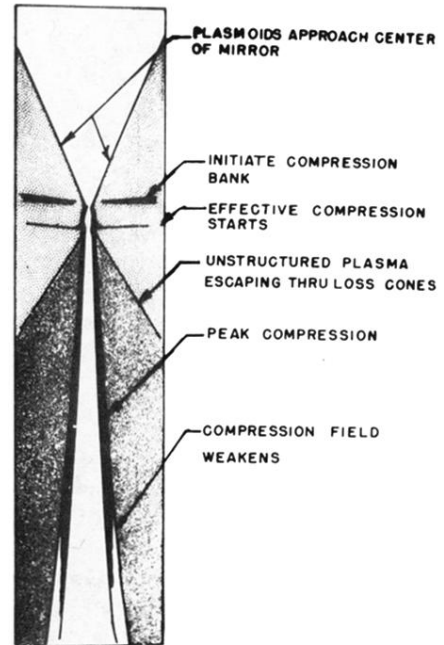
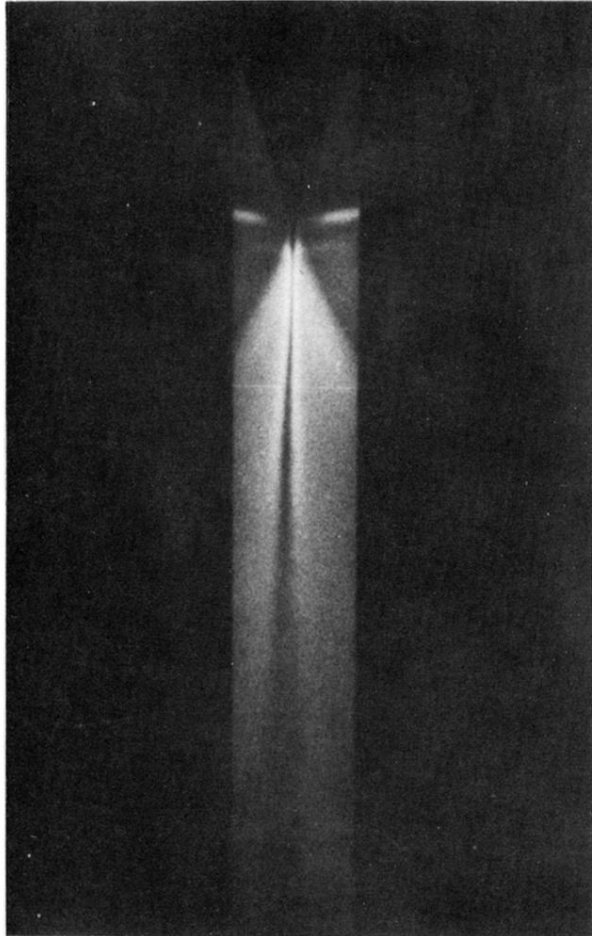


FIG. 2. Streak picture and schematic diagram illustrating collision of vortex structures at center of secondary mirror system. Time goes from top to bottom of the picture and diagram. Streak time is  $50 \mu\text{sec}$ . The horizontal slit was placed along the centerline of the machine, between the secondary compression coils.